



Cite this: *Lab Chip*, 2016, 16, 4702

# Spatiotemporal control of kinesin motor protein by photoswitches enabling selective single microtubule regulations†

K. R. Sunil Kumar, Ammathnadu S. Amrutha and Nobuyuki Tamaoki\*

Artificial control of bio-nanomachines should have a major impact on the development of controllable transport systems for specific cargo transport on chips. Precise spatiotemporal control and local regulation of the bio-motor activity will, however, be necessary if we are to accomplish such a goal. In this study, we exploited the photoswitching properties of azobenzene-based high-energy molecules and inhibitors to control a single kinesin-driven microtubule that has potential to work as a nanocarrier for molecular cargos. In particular, we could influence the local concentration and dispersion of the microtubules at any desired position and time by irradiating a local area of the motility system at one wavelength, while irradiating the entire area at another wavelength, to enrich either *cis* or *trans* isomers of photoswitches in the selected region. Furthermore, various regulations (*e.g.*, transporting, bending, breaking) of single microtubules were possible while almost arresting ambient microtubules—all without the need for any surface patterning.

Received 31st August 2016,  
Accepted 19th October 2016

DOI: 10.1039/c6lc01098a

[www.rsc.org/loc](http://www.rsc.org/loc)

## Introduction

Nano-biomolecular machines (*e.g.*, kinesin, dynein, myosin) fulfill various mechanical functions (*e.g.*, intracellular transport, muscle contraction) of cells by taking advantage of the chemical energy released from the hydrolysis of adenosine triphosphate.<sup>1–3</sup> The motor protein kinesin operates in association with microtubules, tube-like well-defined structures of tubulin proteins having an outer diameter of 25 nm, to transport cell cargos (*e.g.*, vesicles, chromosomes, organelles) to specific sites.<sup>4</sup> The transport behavior, performance, and fuel efficiency of these bio-machines far exceed those of man-made motors when operated on the nanometer scale. Artificial systems based on motor proteins hold significant promise as transport systems for controlled delivery of cargo on chips, with applications in transportation, separation, mixing, and concentration of nano-objects.<sup>5–15</sup> Over the past decade, reverse gliding motility assay systems have been applied successfully to use microtubules as nanocarriers to load, unload, and transport various kinds of cargos (DNA molecules,<sup>16</sup> catalysts,<sup>17</sup> quantum dots,<sup>18,19</sup> gold particles<sup>20</sup> and viruses<sup>21</sup>) on surfaces coated with kinesin motors. The development of such prospective transport systems will be fulfilled, however, only when their individual cargos can be freely selected and

regulated at will. To achieve this, it is important to control the motility of the motor protein in a spatiotemporal manner.

Vogel *et al.* and Tatsu *et al.* reported the use of light-activated release of ATP<sup>22,23</sup> and inhibitors<sup>24</sup> to regulate the kinesin motor activity. However, fast diffusion of the species is a major drawback of the one-way switching property in these systems. This makes it difficult to activate the limited area and to switch the systems back to their initial state. Concerning reversible switching systems, Dekker *et al.*, Hancock *et al.* and Hong *et al.* used micro-electrodes to control and selectively localize the microtubule translocation *via* electric fields.<sup>25–27</sup> Diez *et al.* attempted to regulate the biomolecular activity locally by introducing a thermoresponsive poly(*N*-isopropylacrylamide) surface.<sup>28</sup> Hancock *et al.* and Winter *et al.* examined the directional control of the gliding microtubules using magnetic fields.<sup>29,30</sup> However, the above methods failed to demonstrate complete reversibility. In particular, the OFF state of the motility was hard to achieve. In some cases, the detachment of microtubules from the surface was observed. Furthermore, some surface modifications of the microtubules, which make the fabrication process complicated, were also needed in order to make them responsive to the magnetic field. Apart from these, the above systems relied on the patterned electrode, polymers or magnetic head on the surface of the substrate used as the stimulus platforms to regulate the motility. These stimulus platforms were made to be fixed on the surface, which hampers the free spatial regulation. Therefore, with these methods, it was hard to freely select any particular cargo-carrying microtubules and

Research Institute for Electronic Science, Hokkaido University, N20, W10, Kita-Ku, Sapporo, Hokkaido 001-0020, Japan. E-mail: [tamaoki@es.hokudai.ac.jp](mailto:tamaoki@es.hokudai.ac.jp)

† Electronic supplementary information (ESI) available. See DOI: 10.1039/c6lc01098a



handle them in a controllable manner at any desired position and time.

Recently, we demonstrated the reversible regulation of the motility of microtubules on kinesin using an azobenzene-based photoresponsive high-energy molecule—an azobenzene-derived non-nucleoside triphosphate (AzoTP)—as a substrate instead of ATP<sup>31</sup> and an azobenzene-tethered peptide (Azo-peptide) as a photoresponsive inhibitor of kinesin's motor activity.<sup>32</sup> In both studies, photoisomerization between the *cis* and *trans* forms of these azobenzene groups modulated the activity of the high-energy substrate or inhibitor reversibly by irradiation with two different wavelengths of light.

In this study, we regulated the transportation of selected single microtubules at any desired position and time. The key strategy is to use an optical set-up selectively illuminating areas at two different wavelengths with new photoswitchable agents, enabling the deactivation of the diffused agents by the backward photoisomerization. Hence, we could successfully demonstrate the local concentration, dispersion, and selective regulation of single microtubules (*e.g.*, transporting, bending, and breaking) at any desired position and time on plain glass substrates without any surface patterning.

## Materials and methods

### Chemicals

All chemicals, solvents and reagents were purchased from commercial sources (Tokyo Chemical Industry Co., Ltd., Watanabe Chemical Industries, Ltd., Wako Pure Chemical Industries, Ltd. and Dojindo Molecular Technologies, Inc.) and used without any further purification.

### AzoTP

The non-nucleoside triphosphate (AzoTP) was synthesized and characterized as reported earlier (see the ESI†).<sup>31</sup>

### Azo-peptide

4-((4-Methoxyphenyl)diazanyl)benzoic acid was synthesized by following a previously reported procedure.<sup>33</sup> It was then coupled at the N-terminus of the peptide sequence I-P-K-A-I-Q-A-S-H-G-R, synthesized through an Fmoc solid phase peptide synthesis method, as reported.<sup>32</sup> The coupled product was cleaved from the peptide resin using reagent K (trifluoroacetic acid/phenol/thioanisole/water/triisopropylsilane = 8.25:0.5:0.5:0.5:0.25), purified through HPLC, and analyzed using mass spectrometry [ESI-TOF MS:  $m/z$  1415.40 [ $M + H$ ]<sup>+</sup> (calcd. 1415.75)] (Fig. S2 in the ESI†).

### Instrumentation

Peptide purification and analysis were performed using a Shimadzu reversed-phase (RP) HPLC system. Electrospray ionization time-of-flight mass spectrometry (ESI-TOF MS) was conducted by using a JMS-T100CS instrument (JEOL) in positive ion mode. Absorption spectra were recorded using an Agilent 8453 single-beam spectrophotometer. NMR spectra

were recorded using a 400 MHz spectrometer (ECX-400; JEOL).

### Protein purification and preparation

The kinesin employed in this study was a recombinant kinesin consisting of 573 amino acid residues from the N-terminus of a conventional human kinesin. This recombinant kinesin, fused with His-tag at the N-terminus (plasmid; pET 30b), was expressed in *Escherichia coli* Rossetta (DE3) pLysS and purified through the general method using Ni-NTA-agarose. Tubulin was purified from porcine brains through two cycles of polymerization/depolymerization in the presence of a high-molarity PIPES buffer. Microtubules (MTs) were polymerized using the purified tubulin and labeled with CF 633 succinimidyl ester.

### Optical set-up

To locally regulate the motility of kinesin-driven microtubules, we developed an optical set-up, which allowed irradiation of a particular wavelength of light at the local area of the sample with complete control over its size and position. Fig. 1A provides a schematic representation of our experimental set-up. It shows (i) a sample flow cell chamber containing surface-adsorbed kinesin, fluorescently (CF 633 succinimidyl ester) labeled microtubules, and AzoTP or the Azo-peptide and ATP (placed over an inverted fluorescence optical microscope), (ii) 640 nm excitation light passing through the objective lens for imaging (bottom), (iii) a 488 nm or 365 nm light source (top), (iv) a 365 or 510 nm light source (side), (v) a pinhole of appropriate size, (vi) an XY stage, and (vii) a condenser lens fixed under the XY stage. With this set-up, when we irradiated 488 or 365 nm light from the top, only a small portion of the irradiated light passed through the pinhole, was confined at the condenser lens and spotted onto the sample area. The images in Fig. 1C show the spot size of 488 nm light with a diameter of 18  $\mu$ m (left) and 365 nm light with a diameter of 5  $\mu$ m (right) along with the gliding microtubules. The positions of the light spots were freely moved to other sites of the sample viewing area by turning the screws of the XY stage. The simultaneous irradiation with 510 or 365 nm light from the side covered the entire imaging area of the sample.

### Light irradiation

Surfaces were irradiated with a Hamamatsu LED controller (model C11924-101) for 365 nm light, a Hayasaka LED controller (model CS\_LED 3W\_510) for 510 nm light, and an argon-ion laser source for 488 nm light.

### Fluorescence imaging

Imaging was performed using an inverted fluorescence optical microscope (Olympus, IX-71) equipped with a 100 $\times$ /1.30 NA or 60 $\times$ /1.45 NA oil-immersion objective lens (Olympus), with 640 nm excitation light from a mercury lamp



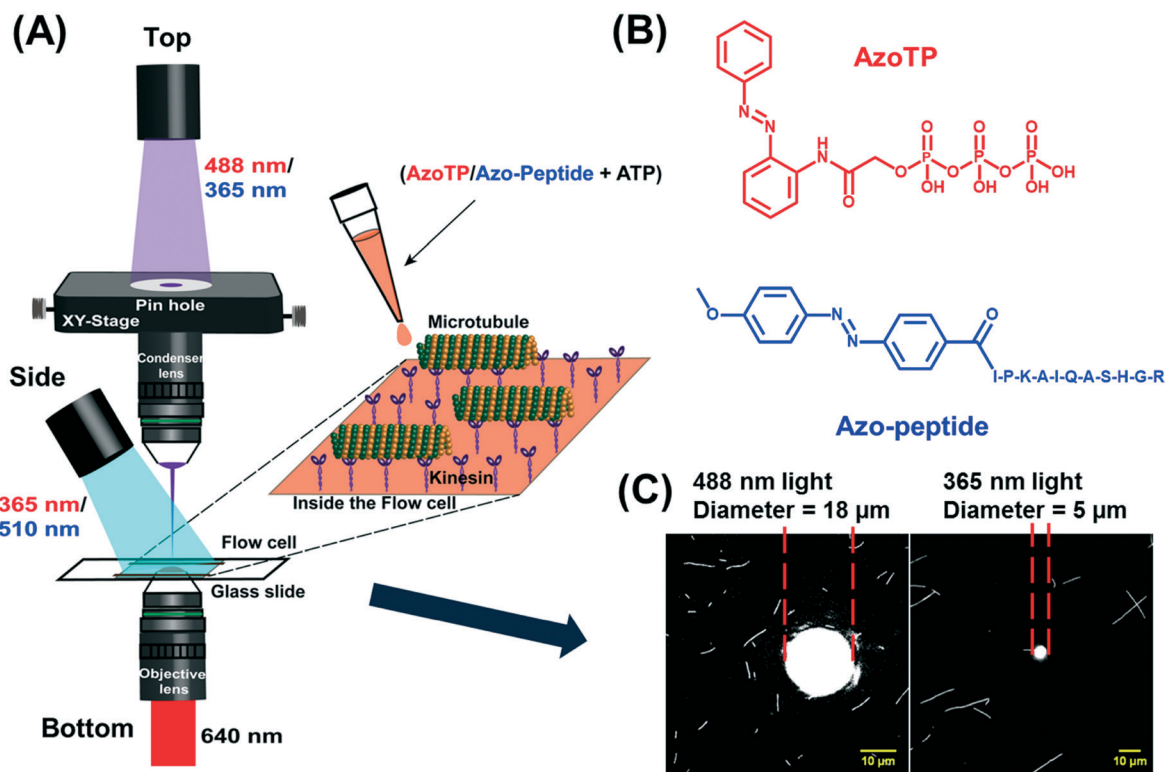


**Fig. 1** (A) Schematic representation of the fluorescence optical microscopy set-up for *in situ* photocontrol over kinesin-driven microtubule motility. (B) Chemical structures of AzoTP and Azo-peptide. (C) Images showing the spot size of the local light irradiation along with the gliding microtubules over a kinesin-coated glass substrate [white circular areas: regions of 488 nm (diameter: 18  $\mu\text{m}$ ) and 365 nm (diameter: 5  $\mu\text{m}$ ) light].

transmitted through appropriate filters. All fluorescence images were recorded using a digital EMCCD camera (model DL-604 M-0EM-H1; ANDOR Solis Technology) and processed using ImageJ software.

### Concentration and dispersion of the microtubules

The flow cell chamber for microscopic observation was prepared by taping a cover slip (18  $\times$  18 mm) and a glass slide (76  $\times$  26 mm) together at both extremities to make a flow path (*ca.* 2  $\times$  18 mm) with a height of *ca.* 100  $\mu\text{m}$ . Furthermore, we didn't perform any microfabrication. The kinesin solution containing casein (3.0  $\mu\text{L}$ ; kinesin: *ca.* 0.125 mg  $\text{mL}^{-1}$ ; casein: 0.5 mg  $\text{mL}^{-1}$ ) was flowed into the prepared chamber and incubated for 3 min. The fluorescently labeled MT solution (3.0  $\mu\text{L}$ ; MTs calculated as tubulin dimer, 1.5  $\mu\text{M}$ ; taxol, 10  $\mu\text{M}$ ) was then flowed into the chamber and incubated for 3 min, followed by washing with the assay buffer (BRB-80 buffer: PIPES, 80 mM;  $\text{MgCl}_2$ , 2 mM; EGTA, 1 mM) containing taxol (10  $\mu\text{L}$ ; 10  $\mu\text{M}$ ). After the final washing with an assay buffer containing taxol (3.0  $\mu\text{L}$ ), an added oxygen scavenger system (casein, 0.5 mg  $\text{mL}^{-1}$ ; 2-mercaptoethanol, 0.14 M; glucose, 20 mM; catalase, 20  $\mu\text{g mL}^{-1}$ ; glucose oxidase, 100  $\mu\text{g mL}^{-1}$ ; ATP, 1.0 mM) and Azo-peptide (2.5 mM) were perfused into the flow cell chamber and both ends were sealed with vacuum grease. Then it was subjected to fluorescence microscopic observation through a 100 $\times$ /1.30 NA oil-

immersion objective lens. The entire flow cell chamber was irradiated with 365 nm light (*ca.* 368  $\text{mW cm}^{-2}$ ) from an LED source as well as laser light ( $\lambda$  = 488 nm) that had been passed through the pin hole and a 5 $\times$  objective lens (Olympus, NA-0.55) to give a local irradiation area (diameter: 18  $\mu\text{m}$ ; *ca.* 90  $\text{W cm}^{-2}$ ). The site of 488 nm local irradiation could be changed readily to any desired position using an XY-displacement stage. The motility assay was performed at 25  $^\circ\text{C}$ .

### Single microtubule regulation

(1) Using AzoTP: a kinesin solution containing casein (3.0  $\mu\text{L}$ ; kinesin: *ca.* 0.125 mg  $\text{mL}^{-1}$ ; casein: 0.5 mg  $\text{mL}^{-1}$ ) was flowed into the prepared chamber and incubated for 3 min. The fluorescently labeled MT solution (3.0  $\mu\text{L}$ ; MTs calculated as tubulin dimer, 0.025  $\mu\text{M}$ ; taxol, 10  $\mu\text{M}$ ) was then flowed into the chamber and incubated for 3 min, followed by washing with the assay buffer (BRB-80 buffer: PIPES, 80 mM;  $\text{MgCl}_2$ , 2 mM; EGTA, 1 mM) containing taxol (10  $\mu\text{L}$ ; 10  $\mu\text{M}$ ). After the final washing with an assay buffer containing taxol (3.0  $\mu\text{L}$ ), an added oxygen scavenger system (casein, 0.5 mg  $\text{mL}^{-1}$ ; 2-mercaptoethanol, 0.14 M; glucose, 20 mM; catalase, 20  $\mu\text{g mL}^{-1}$ ; glucose oxidase, 100  $\mu\text{g mL}^{-1}$ ) and AzoTP (0.5 mM) were perfused into the flow cell chamber and both ends were sealed with vacuum grease. Then it was subjected to fluorescence microscopic observation through a 60 $\times$ /1.45 NA oil-



immersion objective lens. The flow cell chamber was irradiated with laser light ( $\lambda = 488 \text{ nm}$ ) that had been passed through the pin hole and an MPlan Apo SL 50 $\times$  objective lens to give a local irradiation area (diameter:  $5 \mu\text{m}$ ; *ca.*  $356 \text{ W cm}^{-2}$ ); the entire flow cell area was irradiated with  $365 \text{ nm}$  light (*ca.*  $565 \text{ mW cm}^{-2}$ ). (2) Using Azo-peptide: a kinesin solution containing casein ( $3.0 \mu\text{L}$ ; kinesin: *ca.*  $0.125 \text{ mg mL}^{-1}$ ; casein:  $0.5 \text{ mg mL}^{-1}$ ) was flowed into the prepared chamber and incubated for 3 min. The fluorescently labeled MT solution ( $3.0 \mu\text{L}$ ; MTs calculated as tubulin dimer,  $0.025 \mu\text{M}$ ; taxol,  $10 \mu\text{M}$ ) was then flowed into the chamber and incubated for 3 min, followed by washing with the assay buffer (BRB-80 buffer: PIPES,  $80 \text{ mM}$ ;  $\text{MgCl}_2$ ,  $2 \text{ mM}$ ; EGTA,  $1 \text{ mM}$ ) containing taxol ( $10 \mu\text{L}$ ;  $10 \mu\text{M}$ ). After the final washing with an assay buffer containing taxol ( $3.0 \mu\text{L}$ ), an added oxygen scavenger system (casein,  $0.5 \text{ mg mL}^{-1}$ ; 2-mercaptoethanol,  $0.14 \text{ M}$ ; glucose,  $20 \text{ mM}$ ; catalase,  $20 \mu\text{g mL}^{-1}$ ; glucose oxidase,  $100 \mu\text{g mL}^{-1}$ ; ATP,  $1.0 \text{ mM}$ ) and Azo-peptide ( $2.0 \text{ mM}$ ) were perfused into the flow cell chamber and both ends were sealed with vacuum grease. Then it was subjected to fluorescence microscopic observation through a  $60\times/1.45 \text{ NA}$  oil-immersion objective lens. The flow cell chamber was irradiated with  $365 \text{ nm}$  light that had been passed through the pin hole and an MPlan Apo SL 50 $\times$  objective lens to give a local irradiation area (diameter:  $5 \mu\text{m}$ ; *ca.*  $198 \text{ W cm}^{-2}$ ); the entire flow cell area was irradiated with  $510 \text{ nm}$  light (*ca.*  $26 \text{ mW cm}^{-2}$ ). The motility assays were performed at  $25^\circ\text{C}$ .

## Results and discussion

### Concentration and dispersion of the microtubules

To demonstrate the local concentration and dispersion of the microtubules over the kinesin-coated glass substrate, we first prepared a flow cell chamber to contain surface-adsorbed kinesin ( $0.125 \text{ mg mL}^{-1}$ ), microtubules ( $1.5 \mu\text{M}$ ), oxygen scavengers, ATP ( $1.0 \text{ mM}$ ), and Azo-peptide ( $2.5 \text{ mM}$ ) for analysis under a fluorescence optical microscope. In the presence of *trans*-Azo-peptide, all the microtubules existed in the "stopped" state. Irradiation with light at  $365 \text{ nm}$  induced the *trans*-to-*cis* isomerization of Azo-peptide, resulting in the microtubules then moving at an average velocity of  $0.36 \mu\text{m s}^{-1}$ . While irradiating the entire area of the sample with light at  $365 \text{ nm}$ , a small circular local area (diameter:  $18 \mu\text{m}$ ) of the sample was irradiated with light from an  $\text{Ar}^+$  ion laser at  $488 \text{ nm}$ . The resulting local *cis*-to-*trans* isomerization of Azo-peptide induced by the  $488 \text{ nm}$  light completely stopped the motility of the microtubules in that small area. Upon continuing irradiation with both  $365$  and  $488 \text{ nm}$  light, the microtubules under the  $365 \text{ nm}$  light moved at an average velocity of  $0.36 \mu\text{m s}^{-1}$  until they eventually entered the region of  $488 \text{ nm}$  light, whereupon they suddenly stopped moving. After a certain time, the number of microtubules in the  $488 \text{ nm}$  light-irradiated area had significantly increased relative to that in the surrounding area irradiated with  $365 \text{ nm}$  light. Hence, we had established a higher concentration of microtubules in that local area. Furthermore, these microtubules

could be readily dispersed again merely upon stopping the irradiation with  $488 \text{ nm}$  light. Such cycling between local concentration and dispersion of the microtubules could be repeated at any desired site by freely changing the location of the irradiation with  $488 \text{ nm}$  light (see Fig. 2 and Movie S1†). Our method employed here will be a promising tool for the concentration and more sensitive detection of molecules. For example, in homogeneous solution, sensitive detection of the target analyte is quite difficult due to undetectably low quantities. However, such problems can be solved with our new approach where one can concentrate the target analyte and detector molecules loaded on microtubules used as carriers, so that sensitivity for the detection could be enormously increased. Adding reversibility to such systems will make them candidates for recyclable molecular shuttles in future transport systems.

### Selective transportation of a single microtubule

It would be beneficial if one could regulate the movement of a single microtubule in an ensemble, thereby potentially controlling the activity of individual shuttles carrying cargos in future transportation systems. Thus, we examined the potential of our system to selectively transport a single microtubule by exploiting the photoswitching abilities of AzoTP and Azo-peptide. First, we prepared a flow cell chamber to contain surface-adsorbed kinesin ( $0.125 \text{ mg mL}^{-1}$ ), microtubules ( $0.025 \mu\text{M}$ ), oxygen scavengers, and AzoTP ( $0.5 \text{ mM}$ ) for analysis under a fluorescence optical microscope. We illuminated the whole sample area of the flow cell with  $365 \text{ nm}$  light while, at the same time, irradiating a small area (diameter:  $5 \mu\text{m}$ ), containing a selected single microtubule, with light at  $488 \text{ nm}$ . The resulting generation of *cis*-AzoTP under the  $365 \text{ nm}$  light allowed those microtubules to move at only negligible speed ( $0.019 \mu\text{m s}^{-1}$ ), whereas the *trans*-AzoTP photo-generated under the  $488 \text{ nm}$  light induced the selected single microtubule to move forward at a velocity of  $0.101 \mu\text{m s}^{-1}$ . As the selected microtubule moved, we progressively translocated the position of irradiation with  $488 \text{ nm}$  light to maintain its motion (see Fig. 3 and Movie S2†).

We prepared another flow cell chamber containing surface-adsorbed kinesin ( $0.125 \text{ mg mL}^{-1}$ ), microtubules ( $0.025 \mu\text{M}$ ), oxygen scavengers, ATP ( $1.0 \text{ mM}$ ), and Azo-peptide ( $2.0 \text{ mM}$ ) for analysis under a fluorescence optical microscope. We illuminated the whole sample area of the flow cell with  $510 \text{ nm}$  light; simultaneously, we irradiated a selected single microtubule with  $365 \text{ nm}$  light within a circular area having a diameter of  $5 \mu\text{m}$ . Accordingly, *trans*-Azo-peptide was generated under the  $510 \text{ nm}$  light, completely stopping the motility of the microtubules, whereas *cis*-Azo-peptide, photogenerated under the  $365 \text{ nm}$  light, caused the selected single microtubule to move forward. This single microtubule, moving at a velocity of  $0.23 \mu\text{m s}^{-1}$ , could be translocated continuously by progressively changing the position of the irradiating  $365 \text{ nm}$  light (see Fig. 4 and Movie S3†). The observed velocity in this case had an  $\sim 35\%$  difference when





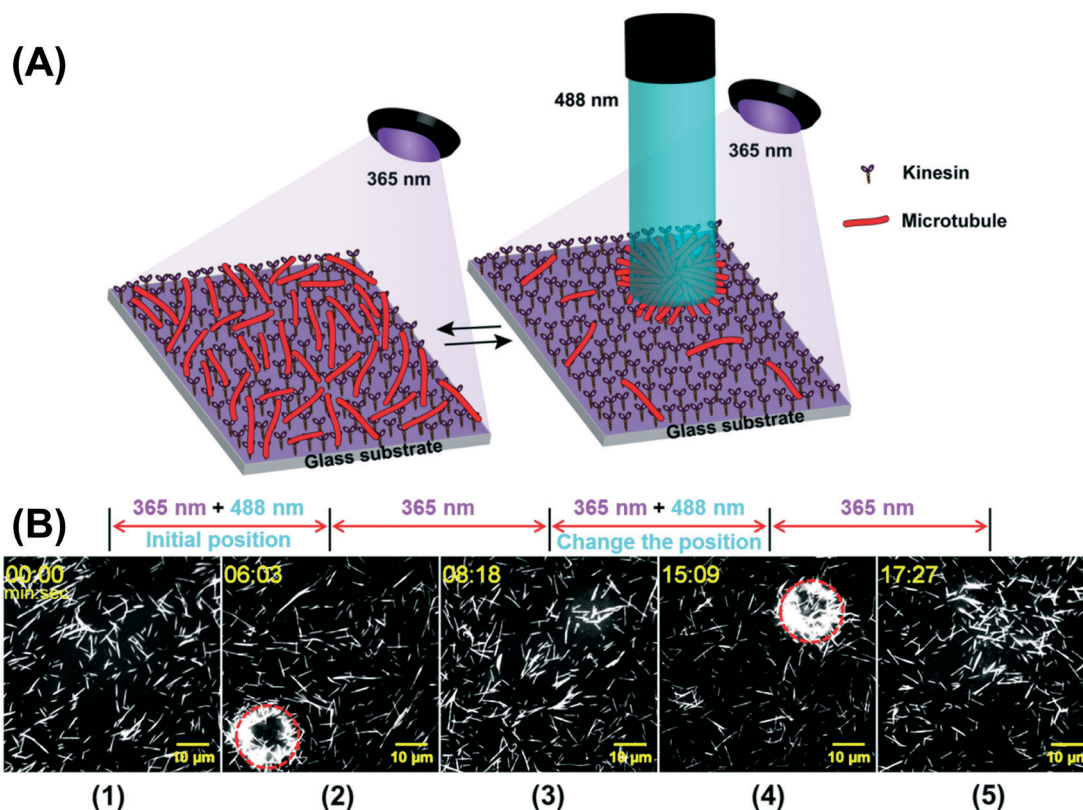


Fig. 2 (A) Schematic representation of the irradiation set-up and the dispersion and concentration of microtubules on a kinesin-coated glass substrate under irradiation with light at 365 and 488 nm. (B) Sequential fluorescence images of gliding microtubules over kinesin in the presence of Azo-peptide (2.5 mM) and ATP (1.0 mM) during the *in situ* photocontrol process: (1) prior to irradiation with 488 nm light; (2) after irradiation with both 488 and 365 nm light for 6 min and 3 s; (3) after terminating irradiation with 488 nm light but maintaining irradiation of the entire imaging area with only 365 nm light for 2 min and 15 s; (4) after changing the location of 488 nm light irradiation and maintaining irradiation of the entire imaging area under 365 nm light for 6 min and 51 s; (5) after terminating irradiation with 488 nm light but maintaining irradiation of the entire imaging area with only 365 nm light for 2 min and 18 s. Red circles: regions of 488 nm light.

compared to that of the microtubule moving under only 365 nm light. This is because of the partial irradiation of 365 nm light at the leading end which covered only ~20% of the microtubule's total length.

These experiments reveal that any specific single microtubule could be selectively transported using either AzoTP or Azo-peptide in conjunction with light of suitable wavelengths. Meanwhile, using AzoTP, we could not completely stop the motility of the microtubules under irradiation with 365 nm light, due to 8% of *trans*-AzoTP being present in the UV photostationary state (PSS) and thereby still inducing motility.<sup>31</sup> Nevertheless, we solved this problem using Azo-peptide, which allowed only the selected microtubule to be transported while almost arresting ambient microtubules. However, in this case, we observed negligibly slower velocity of the surrounding microtubules that might be due to the irradiation with two wavelengths of light. Under such conditions, there exists a new PSS unlike the PSS under only 510 nm light, containing less than 70% of the *trans*-Azo-peptide which is not sufficient to induce a complete “stopped state” of the microtubules. We have also measured the activation profiles for the moving microtubules at a distance away from

the local light illumination area while using Azo-peptide and AzoTP (Fig. S7 and S8†).

So far, selective single microtubule translocation has not been actualized by any other methods. For example, in caged-ATP or caged-inhibitor systems, UV light irradiation induced the release of ATP or inhibitors. Due to fast diffusion, they immediately leave the irradiated area and homogeneously disperse into the solution. Hence, activating a small area was impossible in such systems. Our method has overcome those difficulties using reversible photoswitches. Under local irradiation with 365 or 488 nm light, *trans*-to-*cis* or *cis*-to-*trans* isomerization of the azobenzene groups in Azo-peptide or AzoTP was induced, respectively, at the small area. The simultaneous irradiation with 510 or 365 nm light covering the entire imaging area of the sample induced the *cis*-to-*trans* or *trans*-to-*cis* isomerization of the azobenzene groups in Azo-peptide or AzoTP, respectively, at the surrounding region. Therefore, when Azo-peptide or AzoTP diffused from the local area into the surrounding region, they immediately recovered their original isomeric state. Hence, we could successfully activate the kinesins at a limited area (at least 5 μm) and also selectively induce the motion of a single microtubule.



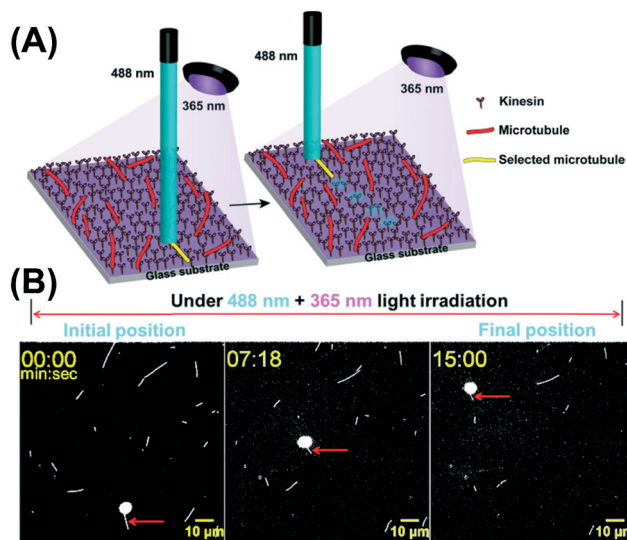


**Fig. 3** (A) Schematic representation of the irradiation set-up for translocation of a single microtubule on a kinesin-coated glass substrate under the influence of light at 488 and 365 nm. (B) Sequential fluorescence images of microtubules gliding over the kinesin-coated surface in the presence of AzoTP (0.5 mM) during the *in situ* photocontrol process at 0 s, 7 min and 18 s, and 15 min. White spots: regions of irradiation with 488 nm light; the entire imaging area was irradiated with light at 365 nm. Red arrows show the position of the translocating microtubule.

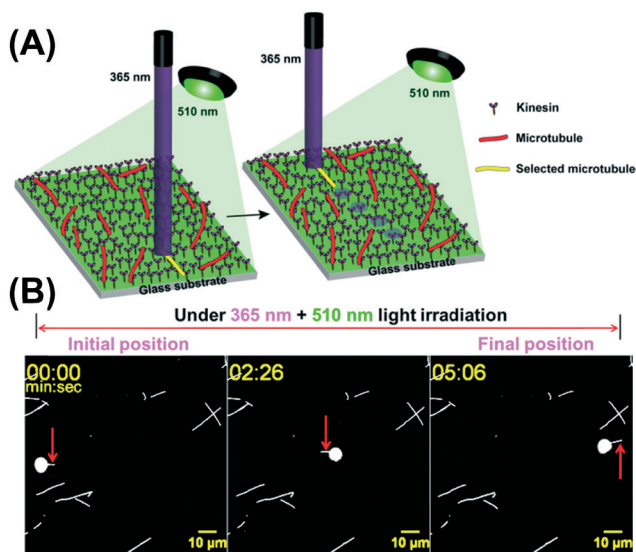


**Fig. 4** (A) Schematic representation of the irradiation set-up and translocation of a single microtubule on a kinesin-coated glass substrate under the influence of light at 365 and 510 nm. (B) Sequential fluorescence images of the gliding of microtubules in the presence of Azo-peptide (2.0 mM) and ATP (1.0 mM) during the *in situ* photocontrol process at 0 s, 2 min and 26 s, and 5 min and 6 s. White spots: regions of 365 nm light; red arrows: position of the translocating microtubule.

Vale *et al.* first reported the novel force-generating motor protein kinesin-promoted linear, ATP-dependent movement of microtubules.<sup>4</sup> Since then, *in vitro* motility assay systems

were extensively studied. However, the role of each kinesin at various sites beneath the single microtubule in inducing the linear motion was still unclear. Using our method, we could locally activate the kinesins, for example, only beneath the leading end of the long microtubule which provided motion to the microtubule. This experimental finding suggested that activation of the kinesins at the leading end of the single microtubule plays a crucial role in driving the linear motion. When we irradiated just at the trailing end, the microtubule couldn't move forward but changed its shape to being bent as shown in the next section. This was also supported by the experiment conducted for the concentration of the microtubules. When the moving microtubules under 365 nm light (kinesin active region) came closer to the local area irradiated with 488 nm light (kinesin inactive region) and hit the boundary with their leading end, they suddenly stopped their motion although the rest of the microtubules lay outside the boundary of the 488 nm light, where kinesins were active under 365 nm light. This gives us clear evidence that the active or inactive state of the kinesins beneath the leading end of the microtubule determines the motion of the microtubule. The rest of the inactive kinesins next to the leading end did not contribute to the motion of the microtubule but just provided support to keep the microtubule on the kinesin surface during transport.

### Bending and breaking of a microtubule

We observed an interesting phenomenon when we used Azo-peptide to selectively regulate a single microtubule of relatively large size. When we irradiated 365 nm light over a circular area (diameter: 5  $\mu\text{m}$ ) covering the trailing end of a microtubule, we detected a change in the shape of the microtubule. Within a few seconds, the central part of the selected microtubule started to bend and, after sufficient bending, it was broken at the site of the bend. We confirmed the breaking of a microtubule by subsequently changing the location of irradiation toward the leading end which moved the microtubule forward, resulting in the separation of the broken parts. In our experiments, we used tunable intensities of the irradiated lights of the background and the local area to limit the active area to the respective sizes of the irradiation spots. Fig. 5 reveals the sequential processes of bending and breaking of the microtubule (also see Movie S4†). This phenomenon was reproducible. We emphasize that the selected microtubule was a single microtubule filament and not the assembled structure of two or three microtubules.

This experiment suggests that local activation of kinesin motors, induced upon irradiation with light at 365 nm, at the trailing end of a microtubule created an internal stress among the tubulin proteins within the microtubule, which was pushed forward from its rear (trailing end) yet blocked from moving at its front (leading end), thereby resulting in a change in shape (bending) and breaking. It is also revealed that the kinesin activation at the leading and trailing ends of the single microtubule has a strong influence on the



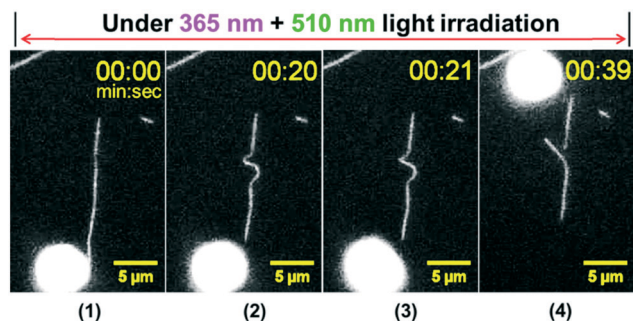


**Fig. 5** Sequential fluorescence images revealing the bending and breaking of a gliding microtubule over a kinesin-coated surface in the presence of Azo-peptide (2.0 mM) and ATP (1.0 mM) during the *in situ* photocontrol process. (1) Initial state; (2) after 20 s of irradiation with both 365 and 510 nm light; (3) after 21 s of irradiation with both 365 and 510 nm light (the microtubule was broken at the centre); (4) after shifting the location of 365 nm light irradiation toward the leading end of the microtubule and maintaining irradiation of the entire imaging area under 510 nm light for 18 s. White spots: regions of 365 nm light.

distinctive mechanical properties of the microtubule such as driving and bending (Movie S4†), which is demonstrated for the first time in the present study of the control of motility with high spatial resolution.<sup>34</sup>

Selective bending and breaking will provide a new insight into understanding the mechanical properties of microtubules and the propulsion power of kinesins. Furthermore, they may help in evaluating the physical properties and the energy for the stability of microtubules at the single molecular level. In addition to its basic scientific importance, breaking a single microtubule would become useful for the advancement of future transport systems. For example, while carrying multiple cargos on a single microtubule, the carrier-breaking technique at the desired position will be useful for site-specific delivery of selected cargos instead of the commonly used unloading method.

## Conclusion

We have demonstrated the controlled local concentration and dispersion of microtubules at any desired position and time without the need for any surface patterning. We have performed several selective and specific regulations of single microtubules, including transporting, bending, and breaking, all under the influence of light. In future studies, we will investigate the possibility of directing single microtubules to desired positions with steering the microtubule either by bending it and making the leading end face the desired direction or by directly guiding it with patterning of light irradiation (e.g., curves, arrows, or other shapes). So far, concerning the first approach, we are, at present, able to change the direction of the linear movement of the microtubule by bending only occasionally without the control to left or right. We anticipate that some specially patterned activation (not the simple circular activation at present) of kinesins with advanced optical set-ups and photomasks for the light

pathways will make it possible to actualize the controlled bending and direct guiding.

## Acknowledgements

We sincerely thank Prof. Takashi Kamei of Hokuriku University for kindly providing human kinesin-1 and CF 633 succinimidyl ester-labeled tubulin. We also thank Md. Jahurul Islam for providing AzoTP and Prof. Hidekazu Kumano of RIES, Hokkaido University for his help in setting up the LA-SER source.

## References

- 1 R. D. Vale, *Science*, 2000, **288**, 88–95.
- 2 R. D. Vale, *Cell*, 2003, **112**, 467–480.
- 3 M. Schliwa and G. Woehlke, *Nature*, 2003, **422**, 759–765.
- 4 R. D. Vale, T. S. Reese and M. P. Sheetz, *Cell*, 1985, **42**, 39–50.
- 5 A. Agarwal and H. Hess, *Prog. Polym. Sci.*, 2010, **35**, 252–277.
- 6 G. D. Bachand, N. F. Boussein, V. Vandelinder and M. Bachand, *Wiley Interdiscip. Rev.: Nanomed. Nanobiotechnol.*, 2014, **6**, 163–177.
- 7 D. J. G. Bakewell and D. V. Nicolau, *Aust. J. Chem.*, 2007, **60**, 314–332.
- 8 T. Fischer, A. Agarwal and H. Hess, *Nat. Nanotechnol.*, 2009, **4**, 162–166.
- 9 A. Goel and V. Vogel, *Nat. Nanotechnol.*, 2008, **3**, 465–475.
- 10 H. Hess, G. D. Bachand and V. Vogel, *Chem. – Eur. J.*, 2004, **10**, 2110–2116.
- 11 M. G. L. van den Heuvel and C. Dekker, *Science*, 2007, **317**, 333–336.
- 12 S. Aoyama, M. Shimoike and Y. Hiratsuka, *Proc. Natl. Acad. Sci. U. S. A.*, 2013, **110**, 16408–16413.
- 13 Y. Hiratsuka, T. Tada, K. Oiwa, T. Kanayama and T. Q. P. Uyeda, *Biophys. J.*, 2001, **81**, 1555–1561.
- 14 T. Kim, L.-J. Cheng, M.-T. Kao, E. F. Hasselbrink, L. Guo and E. Meyhöfer, *Lab Chip*, 2009, **9**, 1282–1285.
- 15 C. T. Lin, M. T. Kao, K. Kurabayashi and E. Meyhofer, *Nano Lett.*, 2008, **8**, 1041–1046.
- 16 S. Diez, C. Reuther, C. Dinu, R. Seidel, M. Mertig, W. Pompe and J. Howard, *Nano Lett.*, 2003, **3**, 1251–1254.
- 17 Y. Jia, W. Dong, X. Feng, J. Li and J. Li, *Nanoscale*, 2015, **7**, 82–85.
- 18 S. Taira, Y. Z. Du, Y. Hiratsuka, T. Q. P. Uyeda, N. Yumoto and M. Kodaka, *Biotechnol. Bioeng.*, 2008, **99**, 734–739.
- 19 L. Rios and G. D. Bachand, *Lab Chip*, 2009, **9**, 1005–1010.
- 20 C. Brunner, C. Wahnes and V. Vogel, *Lab Chip*, 2007, **7**, 1263–1271.
- 21 G. D. Bachand, S. B. Rivera, A. Carroll-Portillo, H. Hess and M. Bachand, *Small*, 2006, **2**, 381–385.
- 22 H. Hess, J. Clemmens, D. Qin, J. Howard and V. Vogel, *Nano Lett.*, 2001, **1**, 235–239.
- 23 R. Tucker, P. Katira and H. Hess, *Nano Lett.*, 2008, **8**, 221–226.
- 24 A. Nomura, T. Q. P. Uyeda, N. Yumoto and Y. Tatsu, *Chem. Commun.*, 2006, 3588–3590.
- 25 C. Van den Heuvel, M. G. L. De Graft and M. P. Dekker, *Science*, 2006, **312**, 910–914.





- 26 M. Uppalapati, Y. M. Huang, T. N. Jackson and W. O. Hancock, *Small*, 2008, **4**, 1371–1381.
- 27 E. Kim, K.-E. Byun, D. S. Choi, D. J. Lee, D. H. Cho, B. Y. Lee, H. Yang, J. Heo, H.-J. Chung, S. Seo and S. Hong, *Nanotechnology*, 2013, **24**, 195102.
- 28 C. Reuther, R. Tucker, L. Ionov and S. Diez, *Nano Lett.*, 2014, **14**, 4050–4057.
- 29 B. M. Hutchins, M. Platt, W. O. Hancock and M. E. Williams, *Small*, 2007, **3**, 126–131.
- 30 K. D. Mahajan, G. Ruan, C. J. Dorcena, G. Vieira, G. Nabar, N. F. Boussein, J. J. Chalmers, G. D. Bachand, R. Sooryakumar and J. O. Winter, *Nanoscale*, 2016, **8**, 8641–8649.
- 31 N. Perur, M. Yahara, T. Kamei and N. Tamaoki, *Chem. Commun.*, 2013, **49**, 9935–9937.
- 32 (a) K. R. S. Kumar, T. Kamei, T. Fukaminato and N. Tamaoki, *ACS Nano*, 2014, **8**, 4157–4165; (b) A. S. Amrutha, K. R. S. Kumar, K. Matsuo and N. Tamaoki, *Org. Biomol. Chem.*, 2016, **14**, 7121–7370.
- 33 S. Prathap Chandran, F. Mondiot, O. Mondain-Monval and J.-C. Loudet, *Langmuir*, 2011, **27**, 15185–15198.
- 34 M. G. L. Van den Heuvel, M. P. de Graaff and C. Dekker, *Proc. Natl. Acad. Sci. U. S. A.*, 2008, **105**, 7941–7946.

